Received: 30 June 2023 | Accepted: 22 June 2023

DOI: 10.1002/pamm.202300101

PAMM Proceedings in Applied Mathematics and Mechanics

RESEARCH ARTICLE

Lévy-type solutions for buckling of shear deformable unsymmetrically laminated plates with rotational restraints

Philip Schreiber | **Christian Mittelstedt**

Department of Mechanical Engineering, Institute for Lightweight Engineering and Structural Mechanics, Technical University of Darmstadt, Darmstadt, Germany

Correspondence
Philip Schreiber, Department of Mechanical Engineering, Institute for Lightweight Engineering and Structural Mechanics, Technical University of Darmstadt, Otto-Berndt-Straße 2, 64287 Darmstadt, Germany.
Email: philip.schreiber@klub.tu-darmstadt.de

Funding information
German Research Foundation, Grant/Award Number: 421986570

Abstract

The local stability of unsymmetric laminated structures is significantly affected by bending-extension coupling and the comparatively low transverse shear stiffnesses, which have to be included in the structural analysis. If such structures have flat surfaces in segments, they can be investigated with the discrete plate analysis. In this analysis, the individual segments are considered as plates with rotational restraints that represent the supporting effect of the surrounding structure. The aim of this work is to improve the analytical stability of laminated plates. Therefore, Lévy-type solutions for the buckling load of the mentioned laminated plates are considered and refined. This offers exact solutions for unsymmetrical cross-ply laminates as well as antisymmetric angle-ply laminates. In order to show the influence of shear deformations, the solutions for classical laminated plate theory (CLPT), first-order shear deformation theory (FSDT), and third-order shear deformation theory (TSDT) are worked out and compared to each other. In the context of TSDT, a new formulation for the rotational elastic restraint is presented, which affects the rotation and the warping of the plate cross-section. This investigation presents the influence of shear deformations on different laminates and classifies the benefits of the different laminated plate theories with respect to the stability behaviour under different boundary conditions. In addition, the influence of bending-extension coupling on different fibre angles and layer sequences is analysed.

1 | INTRODUCTION

Fibre-reinforced composites are typically used for lightweight structures because of their low density and high strength and stiffness properties. The plate-like layered composites consist of very strong and stiff fibres and a comparatively flexible plastic matrix. Due to the in-plane fibres, the so-called laminates have a low transverse stiffness compared to the in-plane stiffnesses. Therefore, the transverse shear deformations depend significantly on the transverse shear stiffness in addition to the laminate thickness. There are different laminated plate theories available for describing the cross-sectional deforma-

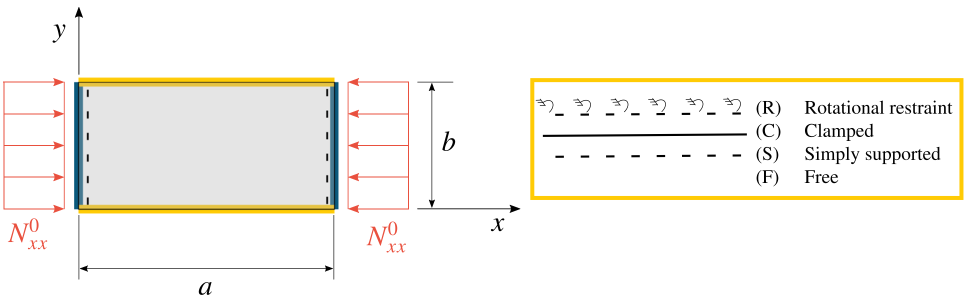

FIGURE 1 Lévy-type boundary conditions with two simply supported edges under a compressive load N_{xx}^0 and two arbitrarily supported edges. The considered laminated plate has the length a and the width b.

tion. The most common is the classical laminated plate theory (CLPT), which neglects the transverse shear deformations, that is, the cross-section remains flat and perpendicular to the mid-plane, see [1]. This is fulfilled in a good approximation only for thin laminates. First-order shear deformation theory (FSDT) makes the assumption of constant transverse shear deformations and gives realistic results even for thicker laminates, see [2–4]. Third-order shear deformation theory (TSDT) describes cubic cross-sectional deformations and thus satisfies the stress boundary condition at the surface layers, which is a more realistic model, see [5, 6]. Therefore, the TSDT is also suitable for very thick laminates as well as for laminates with low transverse shear stiffnesses.

Due to the high stiffness and strength properties of laminates, their lightweight construction generally leads to thin-walled structures. One of the requirements for such structures is that they have to be investigated and designed in terms of their stability, which means that linear buckling analyses are performed. One way to do this analytically is the so-called discrete plate analysis, in which the structure is divided into individual plates and the surrounding structure is modelled with rotational elastic restraints. The stiffness of the restraints can be calculated, for example, as in [7]. These calculations can be performed efficiently with analytical methods.

Besides closed-form analytical methods, the so-called Lévy-type solutions are suitable for this purpose. These consider orthotropic laminates with two simply supported edges and two arbitrarily supported edges, as shown in Figure 1. With respect to the stability of plates, uniaxial compression or biaxial compression can be considered. In the context of symmetric laminates, flange buckling of I-beams has been studied in [8, 9], where Lévy-type solutions are presented in the context of CLPT. The cross-ply laminates considered have a rotational elastic restraint and a free edge in addition to the two simply supported edges. Further Lévy-type solutions for CLPT, FSDT, and TSDT are presented in [10, 11]. These provide a direct solution method of the coupled differential equation system and consider the boundary conditions simply supported, fully clamped and free edges. In the framework of TSDT, the publication [12] uses the so-called state space approach to solve the system of differential equations. The approach reduces the system of differential equations to first order and increases the dimension.

For unsymmetric laminates, in addition to the plate differential equations, the coupled in-plane displacement differential equations must now be considered. In the framework of CLPT, a method is presented in [13] that reduces the problem to one higher order differential equation. In [14] a solution for antisymmetric angle-ply laminates is presented in the framework of FSDT. In [15] solutions for CLPT, FSDT and TSDT are presented for antisymmetric cross-ply laminates that use the state space approach.

All the methods mentioned for unsymmetric laminates investigate the boundary conditions simply supported, fixed clamped and free edges. This investigation extends the considerations to rotational elastic restraints. The presented method provides a Lévy-type solution of the critical load and considers unsymmetric cross-ply and antisymmetric angle laminates with rotational elastic restraints in the framework of CLPT, FSDT, and TSDT. The presented method is a short version of [16], detailed information about the method can be found there.

2 LÉVY-TYPE SOLUTION

In order to investigate the influence of the transverse shear deformation, the Lévy-type solutions in the laminated plate theories CLPT, FSDT, and TSDT are considered. These theories differ essentially in their displacement field, which is shown in Equation (1). In CLPT, the assumption is made that the cross-section always remains flat and perpendicular to the mid-plane, even in the deformed state. This means that transverse shear deformation is not considered in the analysis. The FSDT, conversely, enables the cross-sectional rotation in the form of a variable. In the TSDT, a cubic deformation of the cross-section is permitted, which allows the cross-section to rotate and warp at the same time:

$$
\begin{aligned}
\text{CLPT}: \quad & u(x,y,z) = u_0(x,y) - z\frac{\partial w_0(x,y)}{\partial x}, \\
& v(x,y,z) = v_0(x,y) - z\frac{\partial w_0(x,y)}{\partial y}, \\
& w(x,y,z) = w_0(x,y). \\
\text{FSDT}: \quad & u(x,y,z) = u_0(x,y) + z\psi_x(x,y), \\
& v(x,y,z) = v_0(x,y) + z\psi_y(x,y), \\
& w(x,y,z) = w_0(x,y). \\
\text{TSDT}: \quad & u(x,y,z) = u_0(x,y) + z\psi_x(x,y) - \frac{4z^3}{3t^2}\left(\psi_x(x,y) + \frac{\partial w_0(x,y)}{\partial x}\right), \\
& v(x,y,z) = v_0(x,y) + z\psi_y(x,y) - \frac{4z^3}{3t^2}\left(\psi_y(x,y) + \frac{\partial w_0(x,y)}{\partial y}\right), \\
& w(x,y,z) = w_0(x,y).
\end{aligned}
\tag{1}
$$

The constitutive laws are shown in Equation (2). Compared to the CLPT, the FSDT offers the shear force fluxes in addition to the force fluxes and moment fluxes. The TSDT also has warping moment and higher warping moment fluxes:

$$
\begin{aligned}
\text{CLPT:} \quad & \begin{bmatrix} \underline{N} \\ \underline{M} \end{bmatrix} = \begin{bmatrix} \underline{\underline{A}} & \underline{\underline{B}} \\ \underline{\underline{B}} & \underline{\underline{D}} \end{bmatrix} \begin{bmatrix} \underline{\varepsilon}^{(1)} \\ \underline{\kappa} \end{bmatrix} \\
\text{FSDT:} \quad & \begin{bmatrix} \underline{N} \\ \underline{M} \\ \underline{Q} \end{bmatrix} = \begin{bmatrix} \underline{\underline{A}} & \underline{\underline{B}} & \underline{\underline{0}} \\ \underline{\underline{B}} & \underline{\underline{D}} & \underline{\underline{0}} \\ \underline{\underline{0}} & \underline{\underline{0}} & K\underline{\underline{A}}^{S} \end{bmatrix} \begin{bmatrix} \underline{\varepsilon}^{(1)} \\ \underline{\varepsilon}^{(2)} \\ \underline{\gamma}^{(1)} \end{bmatrix} \\
\text{TSDT:} \quad & \begin{bmatrix} \underline{N} \\ \underline{M} \\ \underline{P} \\ \underline{Q} \\ \underline{R} \end{bmatrix} = \begin{bmatrix} \underline{\underline{A}} & \underline{\underline{B}} & \underline{\underline{E}} & \underline{\underline{0}} & \underline{\underline{0}} \\ \underline{\underline{B}} & \underline{\underline{D}} & \underline{\underline{F}} & \underline{\underline{0}} & \underline{\underline{0}} \\ \underline{\underline{E}} & \underline{\underline{F}} & \underline{\underline{H}} & \underline{\underline{0}} & \underline{\underline{0}} \\ \underline{\underline{0}} & \underline{\underline{0}} & \underline{\underline{0}} & \underline{\underline{A}}^{S} & \underline{\underline{D}}^{S} \\ \underline{\underline{0}} & \underline{\underline{0}} & \underline{\underline{0}} & \underline{\underline{D}}^{S} & \underline{\underline{F}}^{S} \end{bmatrix} \begin{bmatrix} \underline{\varepsilon}^{(1)} \\ \underline{\varepsilon}^{(2)} \\ \underline{\varepsilon}^{(3)} \\ \underline{\gamma}^{(1)} \\ \underline{\gamma}^{(2)} \end{bmatrix}.
\end{aligned}
\tag{2}
$$

The present method describes the buckling shape and buckling load of laminates under compressive load, which have the boundary conditions shown in Figure 1. Out of these, the following two boundary conditions are investigated in more detail. Both laminates are loaded in compression and are simply supported at the loaded edges. The first laminate has additionally rotational elastic restraints at the two unloaded edges and is denoted as SRSR. The second laminate has one free and one rotational restrained edge, this laminate is labelled as SFSR. Furthermore, two different laminate types are considered in this study. Due to the fact that the unsymmetrical cross-ply laminates (CP) and the antisymmetrical angle-ply laminates (AP) have different bending-extension couplings, different in-plane boundary conditions must be established for the purely analytical description of the problem. The boundary conditions for these two cases are given below for the three laminated plate theories considered. At the boundary, $x = 0, a$ applies to the simple support (S):

$$
\left.\begin{aligned}
\text{CP:} \quad & N_{xx}^{0} = v_0 = 0, \\
\text{AP:} \quad & N_{xy}^{0} = u_0 = 0,
\end{aligned}\right\}
\begin{cases}
\text{CLPT:} \quad w_0 = M_{xx}^{0} = 0. \\
\text{FSDT:} \quad w_0 = M_{xx}^{0} = \psi_y = 0. \\
\text{TSDT:} \quad w_0 = M_{xx}^{0} = \psi_y = P_{xx} = 0.
\end{cases}
\tag{3}
$$

At the edges $y = 0, b$, the following applies for the simple support with the rotational restraint (R):

$$\left.\begin{aligned} &\text{CP:}\quad N^0_{yy} = u_0 = 0, \\ &\text{AP:}\quad N^0_{xy} = v_0 = 0, \end{aligned}\right\} \begin{cases} \text{CLPT:} & w_0 = \begin{cases} \left[-M^0_{yy} - k_0 \dfrac{\partial w_0}{\partial y}\right]_{y=0} = 0. \\ \left[M^0_{yy} - k_b \dfrac{\partial w_0}{\partial y}\right]_{y=b} = 0. \end{cases} \\ \text{FSDT:} & w_0 = \psi_x = \begin{cases} \left[-M^0_{yy} + k_0 \psi_y\right]_{y=0} = 0. \\ \left[M^0_{yy} + k_b \psi_y\right]_{y=b} = 0. \end{cases} \\ \text{TSDT:} & \begin{aligned} &w_0 = \psi_x \\ &= \left[\tfrac{4}{3t^2} P_{yy} + k_0\left(-\tfrac{2}{15}\psi_y + \tfrac{1}{5}\tfrac{\partial w_0}{\partial y}\right)\right]_{y=0} \\ &= \left[-\tfrac{4}{3t^2} P_{yy} + k_b\left(-\tfrac{2}{15}\psi_y + \tfrac{1}{5}\tfrac{\partial w_0}{\partial y}\right)\right]_{y=b} \\ &= \left[-M^0_{yy} + \tfrac{4}{3t^2} P_{yy} + k_0\left(\tfrac{8}{15}\psi_y - \tfrac{2}{15}\tfrac{\partial w_0}{\partial y}\right)\right]_{y=0} \\ &= \left[M^0_{yy} - \tfrac{4}{3t^2} P_{yy} + k_b\left(\tfrac{8}{15}\psi_y - \tfrac{2}{15}\tfrac{\partial w_0}{\partial y}\right)\right]_{y=b} \\ &= 0. \end{aligned} \end{cases} \tag{4}$$

At the edge $y = b$ for the free edge (F) the following applies:

$$\begin{aligned} &\text{CP, AP:} \\ &N^0_{yy} = N^0_{xy} = 0, \end{aligned} \begin{cases} \text{CLPT:} & M^0_{yy} = \hat{Q}_y = 0. \\ \text{FSDT:} & M^0_{yy} = M^0_{xy} = Q_y = 0. \\ \text{TSDT:} & \begin{cases} M^0_{yy} - \tfrac{4}{3t^2} P_{yy} = P_{yy} = M^0_{xy} - \tfrac{4}{3t^2} P_{xy} \\ = \tfrac{4}{3t^2}\left(\dfrac{\partial P_{yy}}{\partial y} + 2\dfrac{\partial P_{xy}}{\partial x}\right) + Q_y - \tfrac{4}{t^2} R_y = 0. \end{cases} \end{cases} \tag{5}$$

The governing partial differential equation (PDE) system is given in matrix notation in Equation (6). In the CLPT framework, two in-plane displacement PDEs and one plate PDE describe the problem. The higher laminated plate theories have additionally two PDEs with respect to the two cross-sectional rotations and the full set consists of five coupled PDEs:

$$L_{ij}\Phi_i = 0, \begin{cases} i, j = 1, 2, 3 & \text{for CLPT} \\ i, j = 1, \dots, 5 & \text{for FSDT} \\ & \text{and TSDT} \end{cases} \quad \text{with} \quad \Phi_i = \begin{bmatrix} u_0(x, y) \\ v_0(x, y) \\ w_0(x, y) \\ \psi_x(x, y) \\ \psi_y(x, y) \end{bmatrix}. \tag{6}$$

The ansatz functions are given in Equation (7) and contain the abbreviation $\beta = m\pi/a$. A distinction is made between the CP and AP approaches because the different bending-extension coupling leads to different PDE systems:

$$\Phi_i^{\text{CP}} = \begin{bmatrix} \cos(\beta x) U(y) \\ \sin(\beta x) V(y) \\ \sin(\beta x) W(y) \\ \cos(\beta x) X(y) \\ \sin(\beta x) Y(y) \end{bmatrix}, \quad \Phi_i^{\text{AP}} = \begin{bmatrix} \sin(\beta x) U(y) \\ \cos(\beta x) V(y) \\ \sin(\beta x) W(y) \\ \cos(\beta x) X(y) \\ \sin(\beta x) Y(y) \end{bmatrix}. \tag{7}$$

Due to the fact that the shown approaches from Equation (7) fulfil the boundary conditions and the PDE system from Equation (6) with respect to the variable x, the problem is reduced to an ordinary differential equation (ODE) system which only depends on the variable y. This system is transformed into a first-order system and written in matrix notation in Equation (8), which has a different size depending on the laminated plate theory:

$$\frac{\partial Z_i(y)}{\partial y} = C_{ij} Z_i(y) = 0, \text{with } i, j = 1, \dots, k \begin{cases} k = 8 & \text{for CLPT} \\ k = 10 & \text{for FSDT} \\ k = 12 & \text{for TSDT.} \end{cases} \tag{8}$$

For the first order ODE system from Equation (8) the following solution can be written

$$\underline{Z}(y) = \mathrm{e}^{\underline{\underline{C}}\,y}\,\underline{K} \quad \text{with} \quad \mathrm{e}^{\underline{\underline{C}}\,y} = \underline{\underline{L}} \begin{bmatrix} \mathrm{e}^{\lambda_1 y} & & 0 \\ & \ddots & \\ 0 & & \mathrm{e}^{\lambda_k y} \end{bmatrix} \underline{\underline{L}}^{-1}. \tag{9}$$

Herein, $\underline{K}$ is the vector of constants that could be defined by the boundary conditions. The quantities λ_i are the eigenvalues of $\underline{\underline{C}}$ and $\underline{\mathrm{L}}$ is the matrix of the corresponding eigenvectors. Substituting the approach from Equation (9) into the corresponding boundary conditions from Equations (3, 4, 5) leads to the following homogeneous system of equations:

$$\underline{\underline{M}}\,\underline{K} = 0. \tag{10}$$

For the non-trivial solution of the system of Equations (10), the determinant of the coefficient matrix $\underline{\underline{\mathrm{M}}}$ must vanish. This requirement represents the so-called buckling condition and, in the context of Lévy-type solutions, represents a transcendental equation with respect to the critical buckling load N_{cr}, as shown in Equation (11). This means that the buckling load can only be represented implicitly. For the presentation of the results, this equation is solved iteratively with a numerical roots search:

$$\det\left(\underline{\underline{M}}\right) = 0. \tag{11}$$

However, it turns out that Equation (11) is an ill-conditioned problem. Therefore, the following equivalent substitute problem is considered. In the solution from Equation (9), the component $\overline{\underline{K}}$ is substituted, as shown in Equation (12):

$$\underline{Z}(y) = \underline{\underline{L}} \begin{bmatrix} \mathrm{e}^{\lambda_1 y} & & 0 \\ & \ddots & \\ 0 & & \mathrm{e}^{\lambda_k y} \end{bmatrix} \underbrace{\underline{\underline{L}}^{-1}\,\underline{K}}_{\overline{\underline{K}}} \tag{12}$$

Inserting the approach from (12) into the boundary conditions results in $\overline{\underline{\underline{M}}}\,\overline{\underline{K}} = 0$. The determinant of $\overline{\underline{\underline{M}}}$ gives the new buckling condition, which can be split into a fraction $\underline{\underline{M}}$ and $\underline{\underline{L}}$, as shown in Equation (13).

$$\det(\overline{\underline{\underline{M}}}) = \det(\underline{\underline{M}}\,\underline{\underline{L}}^{-1}) = \frac{\det(\underline{\underline{M}})}{\det(\underline{\underline{L}})} = 0 \tag{13}$$

This substitute problem avoids the calculation of $\underline{\underline{L}}^{-1}$ and has a better condition than the original one. The results presented below use the substitute problem.

3 | RESULTS

The results of the present method are compared with FEA to show that plausible results are obtained. Secondly, different laminate and geometry parameters are investigated. In Figure 2 the non-dimensional buckling load $\overline{N}_{\mathrm{cr}}$ is plotted with

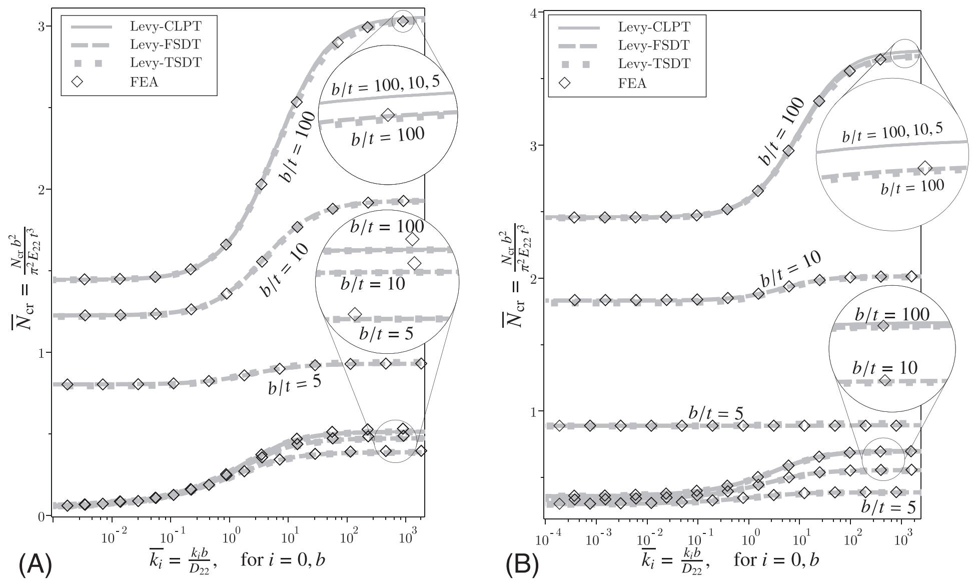

FIGURE 2 The non-dimensional buckling load $\overline{N}_{cr}$ is given as a function of the non-dimensional rotational restraint stiffnesses $\overline{k}_i$ for axial compression, different relative widths b/t (5,10,100) and the boundary conditions SRSR and SFSR with the aspect ratio of $a/b = 10$. (A) Cross-ply laminate $[(0°/90°)_2]$ and (B) Angle-ply laminate $[(45°/-45°)_2]$.

the non-dimensional rotational elastic restraints $\overline{k}_i$ for different relative widths b/t. In the plots, the upper three curves are the results for the SRSR plate and the lower three are those for the SFSR plate. It can be shown that for very thin plates ($b/t = 100$) all laminated plate theories agree with the results of FEA, which uses elements based on the kinematics of FSDT. For smaller relative widths, the CLPT results clearly overstate the buckling loads due to the assumption of neglecting transverse shear rotations. The CLPT curves remain on the upper curve in the non-dimensional presentation. The solutions according to FSDT and TSDT become flatter on the one hand and deliver significantly smaller non-dimensional buckling loads, on the other hand. The antisymmetric cross-ply laminates and angle-ply laminates provide good agreement with the FEA.

In Figure 3 further parameters are investigated including the ply repetition n of the antisymmetric laminate. In Figure 3A the cross-ply laminate showed good agreement for laminates with a high degree of asymmetry ($n = 1$) as well as for symmetrical laminates ($n = \infty$). The change of the aspect ratio a/b shows that the mode change to higher half-wave numbers is well reproduced. The maximum deviations between FEA and Levy-type TSDT solutions are -3.7 % for the SRSR plate and -1.4 % for the SFSR plate. These errors both occur at $n = 1$ and for plates at $a/b = 0.6$ and $a/b = 1$ respectively. In Figure 3B, the fibre angle θ is investigated in addition to n. The agreements of the Lévy-type solution within the TSDT and FEA are very good related to θ, this is valid for the whole range of ply repetitions. For the SRSR plate, the largest deviation of −3.8% occurs at $n = 1$ for a $\theta = 50°$. Here it can be observed that the location of the largest error occurs directly behind a mode change, recognisable by the kink in the curve. The SFSR plate shows no mode change in the considered range of $\theta = 0°, \dots, 90°$ and the error is only −2.2% but at the same location as before.

4 | CONCLUSION

For the antisymmetrical cross-ply laminate, the changes in buckling modes that occur with increasing plate length are reproduced very accurately. For the antisymmetric angle-ply laminates, a very reliable prediction of the buckling load can be given. The individual fibre angles can be represented very well over the range of $0°, \dots, 90°$. The same applies to ply repetitions, which means for a high degree of asymmetry, up to symmetric laminates. For antisymmetrical cross-ply and angle-ply laminates, the FE results agree very well with the Lévy-type solutions.

The comparison of the theories shows a clear overestimation of the buckling load in the framework of the CLPT for small relative widths. The FSDT and TSDT also reproduce small relative widths very well and show comparable results for the critical load in the context of the buckling analysis in the present investigation.

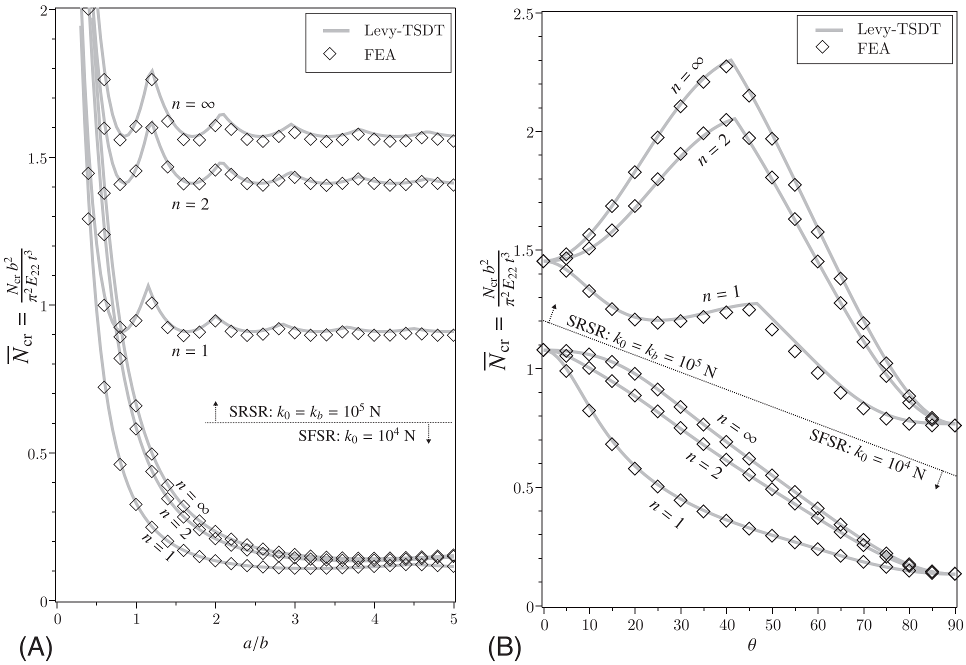

FIGURE 3 Axial compressive loaded laminate with the relative width of $b/t = 10$ and the ply repetitions $n = 1, 2, \infty$ for the boundary conditions SRSR and SFSR with the rotational elastic restraints $k_0 = k_b = 10^5$ N and $k_0 = 10^4$ N, respectively. (A) Cross-ply laminate $[(0°/90°)_n]$: The non-dimensional buckling load $\overline{N}_{cr}$ is given in terms of the aspect ratio a/b. (B) Angle-ply laminate $[(\theta/-\theta)_n]$: The non-dimensional buckling load $\overline{N}_{cr}$ is given in terms of the ply angle θ.

ACKNOWLEDGMENTS

This work was supported by the German Research Foundation (Deutsche Forschungsgemeinschaft, DFG), grant number 421986570.

Open access funding enabled and organized by Projekt DEAL.

ORCID

Philip Schreiber https://orcid.org/0000-0002-3400-0506

REFERENCES

1. Reissner, E., & Stavsky, Y. (1961). Bending and stretching of certain types of heterogeneous aeolotropic elastic plates. *Journal of Applied Mechanics*, *28*(3), 402–408.
2. Yang, P., Norris, C. H., & Stavsky, Y. (1966). Elastic wave propagation in heterogeneous plates. *International Journal of Solids and Structures*, *2*(4), 665–684.
3. Whitney, J. M., & Pagano, N. J. (1970). Shear deformation in heterogeneous anisotropic plates. *Journal of Applied Mechanics*, *37*(4), 1031–1036.
4. Chow, T. S. (1971). On the propagation of flexural waves in an orthotropic laminated plate and its response to an impulsive load. *Journal of Composite Materials*, *5*(3), 306–319.
5. Reddy, J. N. (1984). A simple higher-order theory for laminated composite plates. *Journal of Applied Mechanics*, *51*(4), 745–752.
6. Reddy, J. N. (1984). A refined nonlinear theory of plates with transverse shear deformation. *International Journal of Solids and Structures*, *20*(9-10), 881–896.
7. Qiao, P., & Shan, L. (2005). Explicit local buckling analysis and design of fiber–reinforced plastic composite structural shapes. *Composite Structures*, *70*(4), 468–483.
8. Webber, J., Holt, P. J., & Lee, D. A. (1985). Instability of carbon fibre reinforced flanges of i section beams and columns. *Composite Structures*, *4*(3), 245–265.
9. Bank, L. C., & Yin, J. (1996). Buckling of orthotropic plates with free and rotationally restrained unloaded edges. *Thin-Walled Structures*, *24*, 83–96.
10. Nosier, A., & Reddy, J. N. (1992). On vibration and buckling of symmetric laminated plates according to shear deformation theories: Part I. *Acta Mechanica*, *94*(3–4), 123–144.
11. Nosier, A., & Reddy, J. N. (1992). On vibration and buckling of symmetric laminated plates according to shear deformation theories: Part II. *Acta Mechanica*, *94*(3–4), 145–169.

12. Khdeir, A. A. (1988). Free vibration and buckling of symmetric cross-ply laminated plates by an exact method. *Journal of Sound and Vibrarion*, *126*(3), 447–461.
13. Sharma, S., Iyengar, N., & Murthy, P. N. (1980). Buckling of antisymmetric cross- and angle-ply laminated plates. *International Journal of Mechanical Sciences*, *22*(10), 607–620.
14. Khdeir, A. A. (1989). Stability of antisymmetric angle–ply laminated plates. *Journal of Engineering Mechanics*, *115*(5), 952–962.
15. Reddy, J. N., & Khdeir, A. A. (1989). Buckling and vibration of laminated composite plates using various plate theories. *AIAA Journal*, *27*(12), 1808–1817.
16. Schreiber, P., & Mittelstedt, C. (2023). Lévy-type solutions for the buckling analysis of unsymmetrically laminated plates with rotational restraints for various plate theories. *Archive of Applied Mechanics*, *93*, 2907–2935.

How to cite this article: Schreiber, P., & Mittelstedt, C. (2023). Lévy-type solutions for buckling of shear deformable unsymmetrically laminated plates with rotational restraints. *Proceedings in Applied Mathematics and Mechanics*, *23,* e202300101. https://doi.org/10.1002/pamm.202300101